AGU PUBLICATIONS

JGR

Journal of Geophysical Research: Planets

RESEARCH ARTICLE
10.1002/2013JE004576

Special Section:
Results from the first 360 Sols of the Mars Science Laboratory Mission: Bradbury Landing through Yellowknife Bay

Key Points:
- Introduction to the REMS results on MSL mission
- Overiview of the sensor information
- Overview of operational constraints

Correspondence to:
J. Gómez-Elvira,
gomezej@cab.inta-csic.es

Citation:
Gómez-Elvira, J., et al. (2014), Curiosity's rover environmental monitoring station: Overview of the first 100 sols, *J. Geophys. Res. Planets*, *119*, 1680–1688, doi:10.1002/2013JE004576.

Received 12 NOV 2013
Accepted 15 MAY 2014
Accepted article online 22 MAY 2014
Published online 25 JUL 2014

Curiosity's rover environmental monitoring station: Overview of the first 100 sols

Javier Gómez-Elvira[1], Carlos Armiens[1], Isaías Carrasco[1], Maria Genzer[2], Felipe Gómez[1], Robert Haberle[3], Victoria E. Hamilton[4], Ari-Matti Harri[2], Henrik Kahanpää[2], Osku Kemppinen[2], Alain Lepinette[1], Javier Martín Soler[1], Javier Martín-Torres[1,5], Jesús Martínez-Frías[1,6], Michael Mischna[7], Luis Mora[1], Sara Navarro[1], Claire Newman[8], Miguel A. de Pablo[9], Verónica Peinado[1], Jouni Polkko[2], Scot C. R. Rafkin[4], Miguel Ramos[9], Nilton O. Rennó[10], Mark Richardson[8], José A. Rodríguez-Manfredi[1], Julio J. Romeral Planelló[1], Eduardo Sebastián[1], Manuel de la Torre Juárez[7], Josefina Torres[1], Roser Urquí[11], Ashwin R. Vasavada[7], José Verdasca[1], and María-Paz Zorzano[1]

[1]Centro de Astrobiología (CSIC-INTA), Torrejón de Ardoz, Madrid, Spain, [2]Finnish Meteorological Institute, Helsinki, Finland, [3]NASA Ames Research Center, Moffett Field, California, USA, [4]Southwest Research Institute, Boulder, Colorado, USA, [5]Instituto Andaluz de Ciencias de la Tierra, CSIC-UGR, Armilla, Spain, [6]Instituto Geociencias (GEO-CSIC), Facultad Ciencias Geológicas, Madrid, Spain, [7]Jet Propulsion Laboratory, California Institute of Technology, Pasadena, California, USA, [8]Ashima Research, Pasadena, California, USA, [9]Universidad de Alcalá de Henares, Alcalá de Henares, Spain, [10]University of Michigan, Ann Arbor, Michigan, USA, [11]Ingeniería de Sistemas para la Defensa de España, Madrid, Spain

Abstract In the first 100 Martian solar days (sols) of the Mars Science Laboratory mission, the Rover Environmental Monitoring Station (REMS) measured the seasonally evolving diurnal cycles of ultraviolet radiation, atmospheric pressure, air temperature, ground temperature, relative humidity, and wind within Gale Crater on Mars. As an introduction to several REMS-based articles in this issue, we provide an overview of the design and performance of the REMS sensors and discuss our approach to mitigating some of the difficulties we encountered following landing, including the loss of one of the two wind sensors. We discuss the REMS data set in the context of other Mars Science Laboratory instruments and observations and describe how an enhanced observing strategy greatly increased the amount of REMS data returned in the first 100 sols, providing complete coverage of the diurnal cycle every 4 to 6 sols. Finally, we provide a brief overview of key science results from the first 100 sols. We found Gale to be very dry, never reaching saturation relative humidities, subject to larger diurnal surface pressure variations than seen by any previous lander on Mars, air temperatures consistent with model predictions and abundant short timescale variability, and surface temperatures responsive to changes in surface properties and suggestive of subsurface layering.

1. Introduction

The Rover Environmental Monitoring Station (REMS) on board the Curiosity rover monitors a broad set of environmental parameters. In its first 100 Martian solar days (sols), corresponding to late southern winter and early spring at areocentric solar longitudes $L_s = 151°$ to 208°, REMS performed more than 2.2 million measurements of atmospheric pressure, air and ground temperatures, relative humidity, wind speed and direction, and ultraviolet (UV) radiation simultaneously at an unprecedented frequency of 1 Hz. REMS data are being used to study the meteorology, climate, and habitability of the Curiosity landing site and to compare with results from the landing sites of the Viking landers [*Hess et al*., 1977], Mars Pathfinder [*Schofield et al*., 1997] and Phoenix missions [*Taylor et al*., 2010]. Curiosity's location (4.59°S, 137.44°E) on the floor of Gale Crater (−4.5 km elevation) is substantially different from that of the previous landed missions and provides an opportunity to explore the impact of the significant regional topography on the local atmosphere.

2. Design and Performance of the REMS Sensor Suite

The REMS sensors are located inside the rover chassis (pressure sensors), on two short booms attached to the rover mast at a height of ~1.6 m above the surface (ground temperature, humidity, air temperature, and wind), and on the rover deck (downward UV radiation fluxes) [*Gómez-Elvira et al*., 2012].

The REMS pressure sensor package consists of four Barocap® sensor heads: one with high stability but a longer warm-up time of roughly 150 s and three with less stability but shorter warm-up times of about 1 s. Post landing analysis revealed that the pressure sensors were performing as expected, with pressure being measured with a noise level better than ±0.10 Pa, precision better than ±0.75 Pa and an absolute accuracy better than 3 Pa [*Harri et al*., 2014].

The ground temperature sensor (GTS) is a set of thermopiles oriented such that they view an area of the surface behind and to the right of the rover. The GTS consists of three channels spanning wavelengths of 8–14 μm, 14.5–15.5 μm, and 15–19 μm, but the two longer-wavelength channels are compromised by electronics noise and do not provide useful data. However, the 8–14 μm channel has performed consistent with prelanding expectations of measuring ground brightness temperature with an accuracy of ±4.5 K at 213 K, improving to ±1 K at 273 K [*Gómez-Elvira et al*., 2012].

Relative humidity sensor readings on the Martian surface soon made it clear that the prelaunch calibration parameters had to be revised. The cause is still being studied, but a preliminary recalibration using lab and surface measurements has been developed and gives results consistent with the general behavior expected for a near-equatorial site. More details on the new calibration are given in A.-M. Harri et al. (Mars Science Laboratory: Relative humidity observations: Initial results, submitted to *Journal of Geophysical Research*, 2014).

As discussed in *Gómez-Elvira et al*. [2012], measurements by the REMS air temperature and wind sensors are influenced by the rover structure and waste heat. These sensors are attached to the remote sensing mast (RSM), a ~100 mm diameter metal cylinder which produces both a substantial obstacle to flow and a significant thermal perturbation, and which sits over the rover chassis (atop the rover's thermal plume). The use of duplicate air temperature and wind sensors, located separately on two booms placed 50 mm apart vertically, and 120° apart in azimuth, at ~500 mm above the rover deck, was an attempt to compensate for some of these accommodation problems.

Each air temperature sensor (ATS) consists of a 35 mm long rod with three resistance temperature detector thermistors: one placed at the rod's tip, one a third of the way inward from the tip, and one at its base (in contact with the boom, adjacent to the RSM). Postlanding analysis revealed that both ATSs are performing as expected, with an accuracy better than 5 K and a time response in the range of 20 to 80 s, depending on the natural or forced convection conditions. The use of three thermistors on each rod is needed to assess both the conductive heat transfer along the rod and the boundary layer around the RSM. *Gómez-Elvira et al*. [2012] describe the ambient air temperature retrieval method, which was validated in prelaunch thermal tests. However, one or both ATS may be strongly affected by the flow of heat from the rover's Radioisotope Thermoelectric Generator and/or rover body, depending in part upon the direction of the ambient wind. In addition, depending on time of day, one or both ATS may be in direct sunlight or in shadow. Retrieval of ambient air temperature from ATS measurements was expected to be difficult, even before arrival at Mars. The use of two ATS provides a means of untangling some of these effects, but further calibration and modeling, using, respectively, the REMS wind tunnel and Computational Fluid Dynamics (CFD) simulations, are required (and are ongoing) to improve the quality of the air temperature estimates.

As with the ATS, REMS was designed with a wind sensor on each boom to address some of the accommodation problems. In particular, it was known that the RSM would produce large perturbations (e.g., deflections and/or turbulence) of the ambient air flow when the wind came from behind the wind sensor boom; thus, the two booms were angled at 120° to each other such that at least one sensor would sample a minimally perturbed wind field. The first step in the calibration algorithm designed prior to landing was to examine the wind sensor readings and determine which boom to use, with readings from the other boom then largely ignored. Unfortunately, the wind sensor on boom 1 was found to malfunction upon landing, likely due to damage by surface materials lofted during landing. The boom 2 wind sensor (pointing toward the front of the rover) is performing nominally, but data are only reliable for winds coming from roughly a 180° arc in front of the rover. This constraint is met only a portion of each sol, depending on the circulation and rover orientation. In addition, electronic noise results in unreliable data for temperatures below 213 K, which removes a portion of the diurnal cycle (particularly in the colder seasons). Despite these difficulties, new algorithms have been developed based on CFD models and wind tunnel tests in order to retrieve the maximum amount of wind data from the undamaged boom when conditions are suitable for its use. For the first 100 sols, this results in a daytime and early evening data set with an estimated accuracy of ±50% for wind

speed and ±20° for direction, for about half the potential directions. Although there is no way to repair the damaged boom or to compensate for the noise at low temperature, more data will be returned during warmer periods (i.e., as the mission moves into local summer). The diurnal cycle of wind speeds and directions could be better sampled periodically by changing the rover (and hence boom) orientation when possible (e.g., when parking after a drive).

Six UV sensors are mounted on the rover deck, measuring total irradiance between 200 and 380 nm and within five narrower bands to an accuracy of 10%, as expected [*Gómez-Elvira et al*., 2012]. Collection of direct illumination is limited by the physical aperture of the sensors to within 30° of the normal to the rover deck. Imaging of the sensors indicates that obscuration by dust falling from the atmosphere was not significant during the first 100 sols.

3. REMS in the Context of the Full Mars Science Laboratory Environmental Sensor Suite

In addition to the REMS sensors, further environmental monitoring is performed by the Dynamic Albedo of Neutrons (DAN) instrument, which provides information on the water content of the shallow subsurface [*Mitrofanov et al*., 2012], the Radiation Assessment Detector instrument, which continuously measures the spectrum of high-energy radiation at the surface [*Hassler et al*., 2012, 2014], and by the Sample Analysis at Mars (SAM) instrument, which provide information on the abundance of trace gases at the surface [*Mahaffy et al*., 2013]. Additional information on atmospheric phenomena is provided by various cameras of Mars Science Laboratory (MSL), such as measurements of atmospheric opacity, imaging of cloud motion and estimation of wind direction [*Francis et al*., 2014], image-based searches for dust devils (dust-filled convective vortices), and imaging of aeolian features such as ventifacts and dune fields.

The environmental data set produced by the REMS instrument provides contextual information for measurements performed by other MSL instruments. As one example, changes in the shallow subsurface water abundance as a function of time and location (measured by DAN) can be better interpreted with access to the diurnal cycle of local ground temperature, air temperature, and atmospheric water abundance (measured by REMS). The use of REMS in estimating subsurface properties relevant to such investigations is discussed in this issue in *Hamilton et al*. [2014] and G. M. Martinez et al. (Surface energy budget and thermal inertia at Gale Crater: Calculations from ground-based measurements, submitted to *Icarus*, 2014). As another example, the apparent absence of imaged dust devils in the first 100 sols contrasts with the detection of numerous pressure drops consistent with the passage of convective vortices over the rover, discussed below and in this issue by *Harri et al*., [2014] and *Haberle et al*. [2014]. This result has implications for the overall dustiness of Gale Crater and (in combination with REMS measurements of the thermal environment) contributes to our understanding of dust devil theory and hence of the overall Martian dust cycle. The REMS data for pressure, relative humidity, surface and air temperature, and UV radiation are publicly available through the NASA Planetary Data System. Wind speed and direction will be archived in future data releases after further validation.

4. The REMS Measurement Strategy

Prelanding mission planning using conservative estimates of available payload energy resulted in a baseline strategy for REMS operations that included 5 min of 1 Hz measurements every Mars hour, with an additional hour of REMS 1 Hz measurement during every sol. Once the rover power and thermal subsystems were characterized upon landing, it became clear that additional full hours of REMS measurements were both possible and desirable. While the 5 min hourly measurements are invaluable for providing continuous monitoring of the full diurnal cycle, comparison with extended measurements revealed that the former may not statistically capture the mean and variability of each measured quantity. Given the potential for more REMS monitoring time, the team converged on a strategy that would gradually build up complete coverage of the diurnal cycle over several sols using 1 h "extended blocks" of REMS measurement time. In practice, these were composed of twelve 5 min sessions scheduled consecutively. Shorter extended periods (fewer consecutive 5 min blocks) were also explored, but ultimately, a 1 h extended session was chosen as the standard "unit" of extended time. The main limitations on the number of 1 h extended blocks were energy availability, downlink data volume, the timing and duration of data downlinks and command uplinks, and the

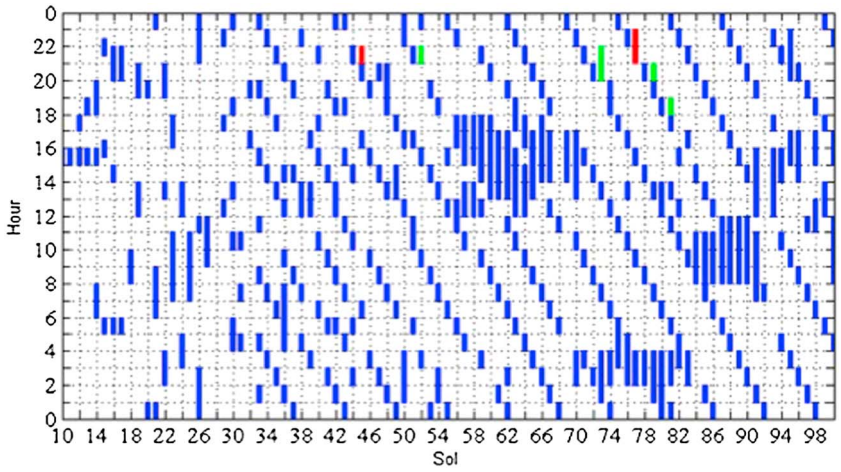

Figure 1. The REMS cadence of 1 h extended blocks (shown in red) for sols 10–100 as a function of local mean solar time (LMST). These were in addition to the regular REMS 5 min blocks at the start of every hour, which are not shown; 15 min, 30 min, and 45 min blocks were also run. "TLS" (green) and "QMS" (red) indicate, respectively, the timing of SAM atmospheric and solid material intake. Some clusters of extended blocks in consecutive sols indicate monitoring of sol-to-sol variability of atmospheric phenomena, such as strong ATS perturbations overnight or in the late morning (sols 70–83 and 84–91, respectively), or the gathering of statistics on pressure drops associated with convective vortices (the noon to 1 P.M. LMST period measured in many sols). Other clusters indicate repeated monitoring of a time period in preparation for a new rover activity, e.g., monitoring of wind speeds and directions between ~1 P.M. and 5 P.M. LMST, prior to the sample dropoff that occurred in sol 98 (see text for more details).

size of the REMS memory cache, which permits a maximum of four 1 h blocks to be stored before transfer of data to the main rover memory is required.

The "REMS cadence" showing REMS extended blocks for the first 100 sols (omitting the first 10 sols when very few REMS measurements were made) is shown in Figure 1. This graphic demonstrates an initial attempt (sols ~30–40) to sample the diurnal cycle with six extended 1 h blocks spaced 3 or 4 h apart, which were shifted 1 h earlier each sol providing full coverage (in 1 h blocks) of the diurnal cycle every 4 sols. Given the limitation on total REMS hours, however, this initial sampling strategy became difficult to maintain in light of other demands on REMS, and the strategy was then changed to four extended 1 h blocks spaced 5 or 6 h apart, providing full extended block coverage of the diurnal cycle in 6 sols. Since sol 100, the REMS cadence has evolved beyond that shown in Figure 1, but we leave its discussion to a future paper. In total, REMS made more than 430 full hours of measurements at 1 Hz during the first 100 sols. During the first 57 sols, the observation blocks had short data gaps as the wind sensors were being characterized using a Wind Sensor (WS)-on/WS-off measuring strategy.

Some of the other aforementioned demands on REMS are also demonstrated in Figure 1. These included REMS science investigations that conflicted with the original cadence, such as a desire to monitor behavior over longer time periods or to study phenomena occurring at certain local times on multiple adjacent sols. The REMS extended blocks have also been used to provide context for other science investigations, such as SAM atmospheric sample analysis where samples of air are captured to measure their composition (shown as "TLS" in Figure 1), MSL imaging campaigns related to atmospheric phenomena (such as searches for dust devils, surface ice, or clouds), or other activities as discussed earlier. In addition, REMS was often requested to provide support for rover operation activities, such as repeated monitoring of the local times when acquired soil or rock powder might be dropped into instrument inlets on the rover deck. Prelanding analysis revealed that sample material was vulnerable to loss during the brief exposure to ambient winds, so REMS data were used to choose optimal dropoff times.

5. Overview of Key REMS Results From the First 100 Sols

This special issue contains papers describing the REMS pressure, relative humidity, near surface air temperature, and ground temperature results from the first 100 sols. The sections below provide highlights from these papers and also briefly discuss preliminary UV and wind results.

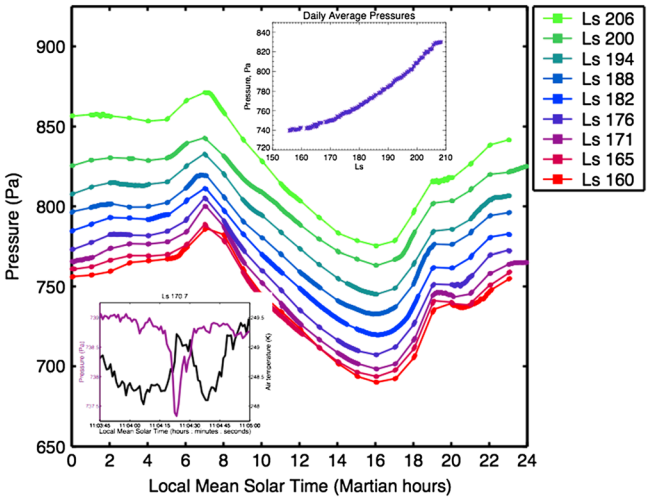

Figure 2. Nine diurnal profiles of pressure showing the seasonal evolution of the diurnal and semidiurnal tides and the rise in pressure due to the sublimation of the southern seasonal polar cap. Secondary peaks between 2:00 and 6:00 LMST, and between18:00 and 20:00 LMST, are unique features of Gale Crater. The top inset shows the seasonal rise in diurnal mean pressure. The bottom inset shows a transient pressure drop (purple) and air temperature peak (black) on sol 37 likely caused by a convective vortex [*Ellehoj et al*., 2010].

6. Surface Pressure

Curiosity landed at the season when the annual pressure cycle is expected to be near its minimum. As shown in this issue by *Harri et al*. [2014], REMS confirmed this by measuring a minimum daily mean surface pressure of 740 Pa at the landing season with pressures increasing by ~1 Pa/sol thereafter. Pressure curves for a few sols are shown in Figure 2. This annual cycle is caused by variations in the global atmospheric mass resulting from the condensation and sublimation of the seasonal CO_2 polar ice caps. The expected long lifetime of the MSL mission and the stability of the pressure sensor will enable REMS to monitor interannual variability in the CO_2 cycle.

The REMS atmospheric pressure sensor has measured diurnal variations of ~90 Pa peak to peak. As shown in this issue by *Harri et al*. [2014] and *Haberle et al*. [2014], these variations represent 12% of the diurnal mean and are larger than those measured by previous landers. Viking Lander 1, for example, found only 2–3% peak-to-peak fluctuations at a similar season. Diurnal pressure variations on Mars are forced mainly by the thermal tides [*Zurek*, 1976; *Tillman*, 1988; *Wilson and Hamilton*, 1996]. Longitudinal variations in topography, surface properties, and atmospheric dust loading can excite eastward propagating Kelvin modes which can interfere with the normal westward propagating Sun-synchronous tide, increasing the daily pressure cycle [*Wilson and Hamilton*, 1996; *Haberle et al*., 2014]. In addition to the tides, a unique aspect of the MSL landing site is the presence of significant regional topography. As demonstrated in Richardson et al. (in preparation, 2014), hydrostatic adjustment flow across this topography in response to the daily cycle of air temperature significantly amplifies the tide amplitudes to generate the large signatures observed.

The REMS pressure sensor also measured very small variations in pressure, fluctuations with amplitudes < 1 Pa and periods between 5 and 10 min, in the early evening of numerous sols. As discussed in *Harri et al*. [2014] and in *Haberle et al*. [2014], these "evening oscillations" may be due to the excitation of gravity waves from developing downslope flows.

Finally, REMS detected a number of transient (lasting ~20 s) pressure drops ranging from 0.5 Pa to 2.5 Pa [*Harri et al*., 2014]; *Haberle et al*., 2014], coinciding with increases in air temperature and changes in wind direction, suggestive of convective vortices. These pressure drops are similar in frequency and magnitude to those measured by the Mars Pathfinder and the Phoenix landers [*Murphy and Nelli*, 2002; *Ellehoj et al*., 2010]. Both of these spacecraft also imaged vortices containing dust ("dust devils"). However, no dust devils were imaged unambiguously by MSL within the first 100 sols, suggesting that typical convective vortices may not be strong enough to lift sufficient dust at Gale.

7. Ground Temperature

As shown in this issue by *Hamilton et al*. [2014], the GTS measured the diurnal ground temperature cycle over the first 100 sols of the mission and found an expected slight increase in amplitude with time as solar insolation increased. The amplitude data cluster into distinct groups corresponding to the locations where the rover was parked for extended periods, indicating different surface properties at those locations. A dust storm near sol 100 also impacted GTS results. Deviations of the observed thermal cycle from the results of idealized models likely reveal heterogeneity within the REMS footprint laterally or with depth. The best fit

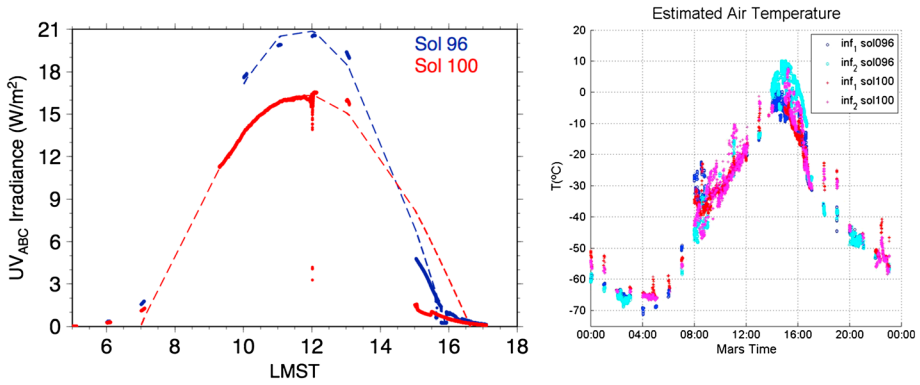

Figure 3. (left) Diurnal cycles of UVABC irradiance on sols 96 and 100, and only the periods on which the sensors measure a mix of direct, diffuse light are shown. Symbols show the observations; dashed lines are a fit to a cosine of the zenith angle to highlight the asymmetry between morning and afternoon hours. On sol 100 the UV sensor was shadowed between 12:15 and 12:25 LMST, causing a drop in the irradiance. Shadowing is also observed on sol 100 near 15:00, and on sol 96 near 16:00 LMST though the irradiance is lower throughout the sol, which is an indication of increased atmospheric opacity. (right) The estimated temperature cycle near each boom for those sols. There is a difference on sol 96 (light and dark blue symbols) between the maximum temperatures near both sensors due to one being shaded and the other one in the Sun. That difference between sensor in the shade and in the Sun disappears on sol 100 (red and pink) due to an increased atmospheric opacity that reduces the impact of the direct solar heating.

thermal inertias obtained with such models are in the range of 230–325 J m^{-2} K^{-1} s$^{-½}$, consistent with surfaces dominated by sand-sized particles and with rover imaging of surface materials.

8. Relative Humidity

As shown in this issue by A.-M. Harri et al. (submitted manuscript, 2014), REMS relative humidity (RH) measurements indicate that the air at the bottom of Gale Crater is rather dry, with the highest measured RH values remaining below saturation even when temperatures are lowest (just before dawn). A clear downward trend in RH after the initial 10 to 20 sols cannot be entirely attributed to the higher nighttime temperatures as the southern hemisphere of Mars moves from winter into spring, indicating a decrease in the absolute water content of the near-surface atmosphere. As yet, it is unclear whether this reflects the rover moving to a different and perhaps drier soil type or a seasonal drying out of the entire region. Further refinement of the calibration and future comparison with ChemCam data [*Meslin et al*., 2013], SAM [*Mahaffy et al*., 2013] and models are expected to help clarify this.

9. Ultraviolet Irradiance at the Surface

Figure 3 shows diurnal cycles of ultraviolet radiation range A, B and C (UVABC) (200–380 nm) on sols 96 and 100. The total irradiance varies from 0 at night to ~ 20 W/m^2 at midday. The noticeable decrease in the daytime UV irradiance from sol 96 to 100 is the result of an increase in atmospheric dust opacity due to a nearby regional dust storm, which also reduced the amplitude of measured ground and air temperatures. The figure also compares the observations to their least squares fit to a cosine of the solar zenith angle. The comparison shows that the UV irradiance curves are asymmetric with respect to maximum solar zenith angle. This could be the result of different atmospheric UV absorption and scattering properties between the morning and afternoon hours, suggesting subdiurnal variability in atmospheric opacities.

Figure 4 shows the evolution of the diurnal maximum value of the total irradiance measured in the UVABC channel. Total irradiance generally increases over the period, as expected for this season. The effects of the regional storm are clearly evident, as well as several transient dips earlier in periods that are associated with more localized changes in the opacity either caused by dust or clouds.

The UV radiation levels are relevant to habitability on the surface and the preservation of organic material. For example, *Chroococcidiopsis* sp. 029, a desiccation-tolerant cyanobacterium, experienced a total loss of viability when exposed to UV dosages at the level measured by REMS [*Cockell et al*., 2005]. Thus, while UV

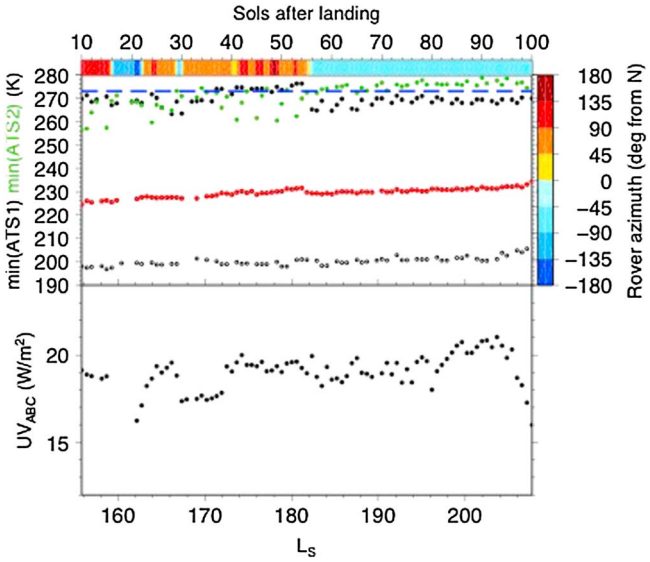

Figure 4. (bottom) Evolution of the maximum diurnal total irradiance (direct plus diffuse) measured by the UVABC channel. (top) Time series of the air temperature maxima from the 5 min average of the minimum thermistor on air temperature sensor 1 (black) and sensor 2 (green). Only maximum daytime temperatures are used from sensor 2 because their nighttime electronic noise results in poor data. The dashed blue line corresponds to 273.15 K; the red symbols are the diurnal mean air temperature measured by sensor 1. To show that differences in the maximum temperatures of each sensor relate to shadowing by the rover; the color bar above the plots indicates the rover orientation where north is azimuth 0°, south is 180°, and east is 90°.

radiation fluxes were found to be below typically used in models of the surface Gale and Mars [e.g., *Haberle et al*., 2013; *Cockell et al*., 2005], the surface environment in Gale Crater is still not favorable for habitability.

10. Air Temperature

Thermal contamination from the radioactive thermal generator, waste heat from the rover, and the influence of solar heating on the ATS all complicate the interpretation of the ATS as an environmental temperature. A heat conduction model was used to estimate the temperatures of the diurnal cycle, and occasionally, as an alternative for analyzing Sun/shadow effects, the minimum value of the sensors on each rod are used as an approximation.

Figure 3 (right) shows the diurnal temperature cycle using the model-estimated true air temperature. Air temperatures do rise above freezing during the day as measured by both air temperature sensors, but we cannot exclude yet that the rate and extent to which this happens is from thermal contamination from the heat generated by the rover. The storm-induced reduction in diurnal amplitude between sol 96 and 100 is readily apparent, however, and is a real consequence of increased dustiness. Maximum air temperatures typically occur after the maximum in UV radiation, as there is a lag between maximum heating and maximum temperatures. The asymmetric shape of the diurnal curves resembles the shape observed by Viking landers. Figure 4 (top) shows the minimum temperature on boom 1 and the maxima on booms 1 and 2. The boom recording the highest maximum switches in several occasions as the rover changes orientation (e.g., on sol 55) represented by the color bar on top of the frames. This figure also shows that the daily average air temperatures monotonically increased ~ 5 K during first 100 sols (Figure 4) as Mars moved closer to the Sun.

11. Wind

New algorithms based on Computational Fluid Dynamics models and wind tunnel tests were developed to retrieve wind information from the undamaged boom. The retrievals are valid only for winds blowing toward the front of the rover and only when ambient temperatures are above −60°C. Under these conditions the estimated accuracy is ±50% for wind speed and ±20° for direction. Therefore, most of the wind data are limited to daytime and early evening and only for slightly above half the potential directions.

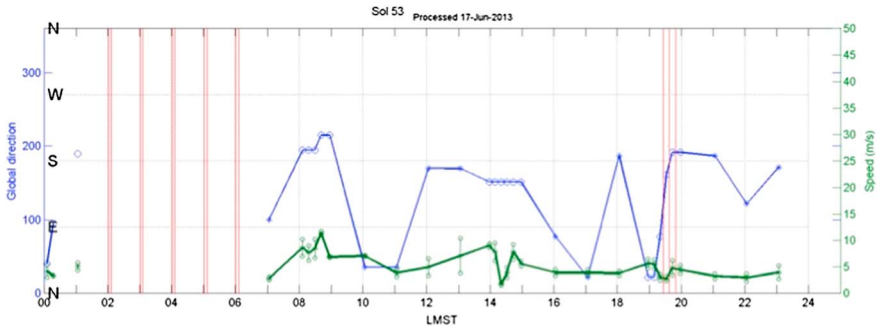

Figure 5. Wind speed and direction are computed second by second and statistically processed hour by hour. The plot represents, in blue, the predominant direction for each hour. The green line connects the mean speeds, indicating around each marker the variability of the standard deviation. A red full line identifies the hours when electronic noise invalidates the readings.

Figure 5 shows the average diurnal cycle of wind speed (green) and direction (blue) as a function of local mean solar time (LMST) for sol 53. Average wind speeds remained typically under 5 m/s. Short-lived wind gusts were also measured and displayed a quasi-repeatable pattern occurring most frequently between 18:00 LMST and 22:00 LMST, although these hours are often subject to high electronic noise. For these hours near sunset, their repeatability and their time coincidence with pressure anomalies suggest a strong correlation with the local topography.

Throughout all 100 sols, a consistent southerly component was observed in the early morning and night, shifting to southwesterly during 18:00–19:00 LMST; this is the direction of Mount Sharp, and the directions, like the timing of the wind gusts, are consistent with what is expected for topographically forced winds. Afternoon winds were mostly easterly, and after sunset they turned southerly. After sol 50, the early morning winds took a northerly component that then split into two preferred modes at 09:00–10:00 LMST centered around the northerly quadrant. Unlike in the first 50 sols, 11:00–13:00 LMST and 16:00–18:00 LMST displayed winds dominated by a northerly component.

12. Conclusions

The REMS instrument suite on MSL is collecting environmental data at a unique site on the surface of Mars. Four of its six sensors are performing as expected while two have required recalibration due to damage (wind sensor) or an unknown reason (humidity sensor). Nevertheless, on its first 100 sols, the REMS sensors have been able to collect information to characterize the details of the diurnal cycles of surface UV radiation, pressure, air temperature (in presence of the rover), surface brightness temperature, relative humidity, and some information about wind directions and speeds.

The REMS UV measurements are the first of its kind and have detected fluxes consistent with the extinction expected from the Martian CO_2 atmosphere and its time-varying dust and clouds. Changes in the ground temperature amplitude suggest that Curiosity traversed through a region of higher inertia materials after leaving Bradbury landing at the beginning of the mission and then entered an area of lower thermal inertia where it stayed until sol 100. REMS detected the largest diurnal pressure variations observed from the surface of Mars consistent with constructively interfering eastward and westward tidal modes possibly enhanced by the local crater circulation. The pressure data also reveal the existence of convective vortices and evening oscillations, with the former generally unable to lift dust and the latter possibly generated by gravity waves. Gale appears to be a very dry environment, which may be a circulation effect, but which could also be due to exchange with an adsorbing or hygroscopic environment. Average winds are moderate with wind gusts frequently occurring after sunset and sunrise. The winds rotated from westerly in the first 50 sols to northerly after sol 50 while keeping a southerly component in the early morning and night hours. Overall, these data do not favor Gale being a habitable environment, at least at the surface. The measured UV dosages sterilize the surface severely limiting the survival rate of simple organisms on its top, and even though ground temperatures exceed the melting point for brief periods during the day, the extremely dry conditions above the regolith would quickly evaporate any surface water whether liquid or ice. As the REMS data analysis

progresses beyond sol 100, it will be able to characterize the influence of seasonal changes on Gale's environment, the impact of dust storms like the one that started around sol 98, and the influence of changing soil properties on the surface brightness temperatures as Curiosity travels through different geological units.

Acknowledgments
We thank the Mars Reconnaissance Orbiter team for sharing information about the southern hemisphere dust storm that occurred around sol 97 of the MSL mission. We also acknowledge the strong support, hard work, and dedication of members of the MSL ENV group responsible for planning environmental observations on MSL. The authors would like to acknowledge financial support provided by the Spanish Ministry of Economy and Competitiveness (AYA2011-25720 and AYA2012-38707) and the Finnish Academy. Part of this research was carried out at the Jet Propulsion Laboratory, California Institute of Technology, under a contract with the National Aeronautics and Space Administration.

References

Cockell, C. S., A. C. Schuerger, E. Daniela Billi, I. Friedmann, and C. Panitz (2005), Effects of a simulated Martian UV flux on the cyanobacterium, Chroococcidiopsis sp. 029, *Astrobiology*, *5*(2), 127–140, doi:10.1089/ast.2005.5.127.

Ellehoj, M. D., et al. (2010), Convective vortices and dust devils at the Phoenix Mars mission landing site, *J. Geophys. Res.*, *115*, E00E16, doi:10.1029/2009JE003413.

Francis, R., J. Moores, K. McIsaac, D. Choi, and G. Osinski (2014), Observations of wind direction by automated analysis of images from Mars and the MSL rover, *Acta Astronaut.*, *94*(2), 776–783.

Gómez-Elvira, J., et al. (2012), REMS: The environmental sensor suite for the Mars Science Laboratory rover, *Space Sci. Rev.*, *170*, 583–640.

Haberle, R. M., et al. (2013), Meteorological predictions for the first 30 Sols of the REMS experiment on MSL, *Mars J.*, in press.

Haberle, R. M., et al. (2014), Preliminary interpretation of the REMS pressure data from the first 100 sols of the MSL mission, *J. Geophys. Res. Planets*, *119*, 440–453, doi:10.1002/2013JE004488.

Hamilton, V. E., et al. (2014), Observations and preliminary science results from the first 100 sols of MSL Rover Environmental Monitoring Station ground temperature sensor measurements at Gale Crater, *J. Geophys. Res. Planets*, *119*, 745–770, doi:10.1002/2013JE004520.

Harri, A.-M., et al. (2014), Pressure observations by the Curiosity rover: Initial results, *J. Geophys. Res. Planets*, *119*, 82–92, doi:10.1002/2013JE004423.

Hassler, D. M., et al. (2012), The Radiation Assessment Detector (RAD) investigation, *Space Sci. Rev.*, *170*, 503–558, doi:10.1007/s11214-012-9913-1.

Hassler, D. M., et al. (2014), Mars' surface radiation environment measured with the Mars Science Laboratory's Curiosity rover, *Science*, *343*, doi:10.1126/science.1244797.

Hess, S. L., R. M. Henry, C. B. Leovy, J. A. Ryan, and J. E. Tillman (1977), Meteorological results from the surface of Mars: Viking 1 and 2, *J. Geophys. Res.*, *82*, 4559–4574, doi:10.1029/JS082i028p04559.

Mahaffy, P. R., et al. (2013), Abundance and isotopic composition of gases in the Martian atmosphere from the Curiosity rover, *Science*, *341*(6143), 263–266, doi:10.1126/science.1237966.

Meslin, P. Y., et al. (2013), Soil diversity and hydration as observed by ChemCam at Gale crater, Mars, *Science*, *341*, doi:10.1126/science.1238670.

Mitrofanov, I. G., et al. (2012), Dynamic Albedo of Neutrons (DAN) experiment onboard NASA's Mars Science Laboratory, *Space Sci. Rev.*, *170*, 559–582, doi:10.1007/s11214-012-9924-y.

Murphy, J., and S. Nelli (2002), Mars Pathfinder convective vortices: Frequency of occurrences, *Geophys. Res. Lett.*, *29*(23, 2103), doi:10.1029/2002GL015214.

Schofield, J. T., J. R. Barnes, D. Crisp, R. M. Haberle, S. Larsen, J. A. Magalhães, J. R. Murphy, A. Seiff, and G. Wilson (1997), The Mars Pathfinder atmospheric structure investigation meteorology (ASI/MET) experiment, *Science*, *278*, 1752–1758, doi:10.1126/science.278.5344.1752.

Taylor, P. A., et al. (2010), On pressure measurement and seasonal pressure variations during the Phoenix mission, *J. Geophys. Res.*, *115*, E00E15, doi:10.1029/2009JE003422.

Tillman, J. E. (1988), Mars global atmospheric oscillations: Annually synchronized, transient normal-mode oscillations and the triggering of global dust storms, *J. Geophys. Res.*, *93*, 9433–9451, doi:10.1029/JD093iD08p09433.

Wilson, R. J., and K. Hamilton (1996), Comprehensive model simulation of thermal tides in the Martian atmosphere, *J. Atmos. Sci.*, *53*, 1290–1326, doi:10.1175/1520-0469(1996)053<3C1290:CMSOTT>3E2.0.CO;2.

Zurek, R. W. (1976), Diurnal tide in the Martian atmosphere, *J. Atmos. Sci.*, *33*, 321–337, doi:10.1175/1520-0469(1976)033<0321:DTITMA>2.0.CO;2.